Semina
Ciências Exatas e Tecnológicas

e-ISSN 1679-0375
PHYSICS

ORIGINAL ARTICLE DOI 10.5433/1679-0375.2023.v44.47835

Recovering the Cathode Material Adhered to the Collector and Separator of Spent Lithium-Ion Batteries for Recycling Purposes

Recuperação do Material Catódico Aderente ao Coletor e Separador de Baterias de Íons de Lítio Descartadas para Fins de Reciclagem

Marcelo Henrique Novaes[1]; Paulo Rogério Catarini da Silva[2]; Paulo Sergio Parreira[3]; Gabriel Gonzaga dos Santos[4]; Lucas Evangelista Sita[5]; Jair Scarminio[6]

ABSTRACT

Depleted Li-ion batteries (LIBs) must be recycled for environmental and sustainability reasons. Most recycling processes are dedicated to the recovery of Li, Co, Mn, and Ni present in the cathode material of LIBs. However, separating the cathode material strongly adhered to the aluminum collector and those mechanically trapped into the polymeric separator is still challenging. Processes to separate the cathode material by dissolving its aluminum collector in NaOH solution and to extract part of this material encrusted in the separator by ultrasonic cavitation and mechanical friction are presented in tests with NMC batteries on a laboratory scale. Tests of LIB discharges were also carried out in different $MnSO_4$ solution concentrations, and the related electrochemical reactions were discussed.

keywords lithium-ion battery, cathode material, separation methods, discharge in solution

RESUMO

Por motivos ambientais e de sustentabilidade, baterias de íon-lítio (BILs) esgotadas devem ser recicladas. A maioria dos processos de reciclagem é dedicada à recuperação de Li, Co, Mn e Ni presentes no material do catodo dos BILs. No entanto, separar o material do catodo fortemente aderente ao coletor de alumínio e aqueles retidos mecanicamente no separador polimérico ainda são desafios. Processos para separar o material do catodo dissolvendo o coletor de alumínio em solução de NaOH e para extrair parte desse material que fica incrustados no separador por cavitação ultrassônica e fricção mecânica são apresentados em testes com baterias NMC, em escala de laboratório. Foram ainda realizados testes de descarregamento de BILs em soluções com diferentes concentrações de $MnSO_4$, e discutidas as reações eletroquímicas relacionadas.

palavras-chave bateria de íons de lítio, material catódico, métodos de separação, descarga em solução

Received: March 27, 2023 *Accepted: October 12, 2023* *Published: November 08, 2023*

[1]Undergraduate Student, Department of Physics, UEL, Londrina, PR, Brazil. E-mail: mhenriquenovaes.1@uel.br
[2]Technician Dr., Department of Physics, UEL, Londrina, PR, Brazil. E-mail: prcsilva@uel.br
[3]Prof. Dr., Department of Physics, UEL, Londrina, PR, Brazil. E-mail: parreira@uel.br
[4]Master Student, Department of Physics, UEL, Londrina, PR, Brazil. E-mail: gabriel.gonzaga@uel.br
[5]PhD student, Department of Physics, UEL, Londrina, PR, Brazil. E-mail: lucas.evangelista@uel.br
[6]Prof. Dr., Physics Dept. UEL, Londrina, Paraná, Brazil. E-mail: scarmini@uel.br

Introduction

Lithium-ion batteries (LIBs) are currently the most employed electrical energy source for mobile devices such as cell phones, notebooks, and medical devices, being progressively employed in large mobile units such as electric vehicles, satellites, and space stations (Mahmud et al., 2022). They are also used as stationary batteries for storing electrical energy from alternative sources, such as solar and wind (Chen et al., 2020). The high volumetric charge density, low specific mass, chemical and thermal stability, rechargeability, and consolidated production chain face the large application spectrum for these batteries.

Consequently, a considerable number of depleted LIBs are continuously generated, considering the finite lifespan of these batteries. The disposal, collection, and processing of depleted LIBs must be correctly managed. Recycling is considered the most suitable process for intelligent and sustainable reuse of various valuable battery material and to avoid negative environmental impacts resulting from inappropriate disposal. Although the recycling of LIBs is already industrially established in several countries, more efficient techniques with lower energy costs and fewer pollutants are still necessary and are continuously being developed (Bae & Kim, 2021; Sita et al., 2022).

A typical LIB comprises a cathode and anode (the electrodes), a polymeric separator mechanically and electrically isolating the two electrodes, and an electrolyte, the source of mobile Li^+ ions between the two electrodes in the charging and discharging processes of the battery (Hu et al., 2022).

The cathode electroactive material is a $LiNi_xMn_yCo_zO_2$ compound, with $0 \leq x, y, z \leq 1$ and $x + y + z = 1$, or a mixture of two or even three of these compounds, such as $LiCoO_2$ (LCO), $LiMn_2O_4$ (LMO), $LiNi_{0.5}Mn_{0.3}Co_{0.2}O_2$ (NMC), and many others. The anode is usually carbonaceous, such as high-purity graphite (Asenbauer et al., 2020).

In cathode manufacture, powder of the electroactive material is mixed with a polymeric binder and spread out to form a layer on an aluminum strip, the collector. After pressing and drying the cathode material layer onto the collector and curing the binder, high adhesion is achieved between the cathode powder particles and the aluminum substrate (Zhong et al., 2021). A similar process is employed to manufacture the anode, resulting in a graphite layer adhered to the copper collector.

The strips of cathode, separator, and anode are wounded and firmly compacted inside the battery case, assuring a volume-to-mass low ratio to the battery. Lithium-ion intercalations during the charge and discharge cycles promote the expansion and contraction of the anode and cathode layers. Consequently, cathode and anode materials are frequently trapped in opposite faces of the separator.

In recycling spent LIBs, the major interest is in the cathode material because it contains valuable metals such as Li, Co, Ni, and Mn. Therefore, extracting as much cathode material as possible from the layer on the Al collector and that encrusted in the polymeric separator is essential. It is noteworthy that in the cathode of a LIB, the two faces of the aluminum collector are covered only by the electroactive material of the cathode. However, one of the separator faces is in contact with the cathode material, while the other is in contact with the anode material (graphite).

Several techniques have been proposed to extract the cathode material from its cathode electrode, such as the chemical dissolution of the binder (generally PVDF) by organic solvents or thermal dissociation (pyrolysis) and the chemical dissolution of the aluminum collector by an aqueous solution of NaOH (Bai et al., 2021; Gaye et al., 2019; He et al., 2021; Hu et al., 2021; Sita et al., 2015).

Tests show that the dissolution of the collector aluminum foil strongly depends on the NaOH concentration (Ferreira et al., 2009), but there is no agreement on whether the reaction time and temperature are significant in the dissolution process (Weng et al., 2013).

A search in the literature did not report methods describing how to release electrode materials embedded in the separator. In recycling methods where many batteries are previously crushed (comminution), mechanical processing stages of the battery fragments release, at least partially, the material trapped in the separator, but not entirely.

Recycling processes on a laboratory scale and even in industrial recycling plants are initiated by discharging the batteries to avoid fire or explosion due to electrolyte combustion (Chen et al., 2021). Among the proposed methods, electrochemical discharge in aqueous salt solutions stands out due to its simplicity, low cost, and operational capacity. However, depending on the solute used, corrosion may occur on the battery's positive pole, causing electrolyte leakage, solution entry into the battery, and precipitating on the cathode pole (Ojanen et al., 2018; Shaw-Stewart et al., 2019; Torabian et al., 2022; Xiao et al., 2020; Yao et al., 2020). Promising results were obtained with $MnSO_4$ solutions enabling battery discharge with low cathode pole corrosion (Xiao et al., 2020; Yao et al., 2020). However, the effects of $MnSO_4$ solution concentration on LIB discharge have only been studied at concentrations above 0.4 mol L^{-1} (Yao et al., 2020).

Under the above considerations, the main objective of this work is to conduct dissolution and ultrasound cavitation tests to assess the parameters that optimize the recovery of the cathode material adhered to the battery cathode and those encrusted into the separator of discarded batteries.

As the batteries should be discharged before dismantling to allow access to their components, a detailed study of LIB discharge was also carried out at $MnSO_4$ solution concentrations and reaction times different from those indicated in the literature to find the range of efficiency of these parameters in the battery discharge. It was also discussed in detail how the electrochemical reactions in the $MnSO_4$ solution promote the battery discharge. The electrode materials resulting from the application of the recovery methods were analyzed by X-ray diffraction (XRD) and X-ray fluorescence by dispersive energy (EDXRF).

Materials and methods

Batteries and discharging tests

Exhausted cylindrical Li-ion batteries of different brands and compositions, with nominal capacities of 2200 mAh/cell, were obtained from a laptop battery pack donated by a local maintenance workshop.

Discharge tests were performed as a function of the concentration of the manganese sulfate solution and the reaction time both in as-received batteries and after charging them to 4.2 V by the CC (550 mA) + CV (4.2 V) protocol. A potentiostat/galvanostat (Arbin Instruments, BT200/MSTAT 8000) was used to charge and discharge the batteries.

Aqueous $MnSO_4$ solutions were prepared at 0.1, 0.5, and 1.0 mol L^{-1}. In the discharges, the solution completely covered the battery under test. The battery discharge state was identified by measuring its voltage at intervals of about 30 minutes by removing it from the solution. The procedure was repeated until the battery voltage dropped to about 2.0 V or less. Discharge tests were performed in duplicate for each solution concentration.

Battery Dismantling and Components

Before opening, the batteries were discharged using the 0.50 mol L^{-1} $MnSO_4$ solution, which was assessed as the optimized concentration for the lowest discharging time, as shown below. The batteries were opened manually by following a process detailed in (Sita et al., 2017), giving access to the roll of electrodes and separator, which were carefully withdrawn and unwound, resulting in isolated strips of the cathode, anode, and separator.

Cathode Material Recovery and Analyses

In extracting the cathode material from its electrode by dissolving the Al collector in NaOH solutions, small pieces of the cathode strip (about 1.0 cm^2 each and weight fixed in 1.5 g) were immersed in solutions of 0.50; 0.75; 1.00; 1.25; 1.50, and 1.75 mol L^{-1} concentrations and reaction times of 1 and 4 hours. In total, 12 dissolution tests were performed at room temperature. An analytical balance (Shimadzu AY220, 0.01 mg resolution) was used for mass mass measurements.

After each dissolution test, the solution was vacuum filtered to separate the undissolved reaction products, which were dried at 80 °C for about 12 h and weighed. The dried residues in which aluminum was not visually observed were pulverized in a mortar and analyzed by energy-dispersive X-ray fluorescence (Shimadzu, EDX-720) to detect the elements in the residue.

The filtered solution was evaporated at 80 °C, and the resulting solid was analyzed by X-ray diffraction. The X'Pert High Score Plus software was used on the X-ray diffraction data to identify the crystalline compounds in the analyte (powder materials) and perform Rietveld refinements determining the compounds' relative weights.

An ultrasonic bath was used to extract electrode materials trapped in the separator. After being removed from the battery, the separators were submerged in distilled water and subjected to ultrasonic cavitation for about 10 minutes at room temperature. The powdered material released from the separator was recovered by evaporating the water. In a second step, the separator was dried, inserted into a plastic bag, and manually rubbed, detaching the material that remained trapped in the separator after the cavitation test.

Results and Discussion

Dissolution of the Aluminum Collector

Table 1 shows the results of the twelve tests carried out to dissolve the aluminum of the cathode collector as a function of NaOH solvent concentration in two reaction times. The fourth column displays the result of visual evaluations for the presence of aluminum in the solution residue obtained by filtering the dissolved solution and drying the residue. The fifth column shows the Al relative weight concentration obtained by EDXRF measurements in six residues of the dissolution reactions, with details found in Table 2, where the presence of Al was not visually observed.

Tests were performed in cells belonging to the same battery pack.

Table 1 - Results of the cathode collector dissolution tests as a function of NaOH concentration, reaction time, and the relative concentration of the aluminum element on the dissolution residue measured by EDXRF.

Test #	Concentration NaOH (mol L^{-1})	Time (h)	Dissolved?	Al mass by EDXRF (%)
1	0.50	1.0	no	Not analyzed
2	0.50	4.0	"	"
3	0.75	1.0	"	"
4	0.75	4.0	"	"
5	1.00	1.0	"	"
6	1.00	4.0	"	"
7	1.25	1.0	yes	35.75
8	1.25	4.0	"	0.0
9	1.50	1.0	"	34.02
10	1.50	4.0	"	0.0
11	1.75	1.0	"	0.0
12	1.75	4.0	"	0.0

Table 2 - Elements and their relative weight obtained by EDXRF measurements in residues of cathodes dissolved in NaOH solution tests described in Table 1.

Element (%)	Test					
	# 7	# 8	# 9	# 10	# 11	# 12
Al	35.75	0.00	34.02	0.00	0.00	0.00
Ni	34.43	55.78	35.47	55.75	55.59	55.45
Mn	16.67	23.42	16.89	23.31	23.47	23.47
Co	13.07	20.80	13.56	20.94	20.89	20.07
Ca	0.06	0.00	0.00	0.06	0.09	0.10

It can be seen that NaOH solution with concentrations below 1.00 mol L^{-1} does not lead to the aluminum collector's complete dissolution, even after four hours of reaction.

At 1.25 and 1.50 mol L^{-1} solution concentrations, aluminum foil can be dissolved into the solution after four hours of reaction, whereas the 1.75 mol L^{-1} solution demands just one hour to dissolve the aluminum collector. Accordingly, the complete dissolution of the cathode collector depends on the NaOH solution concentration and the reaction time.

Figures 1(a)-1(c) display images of #3, #4, and #6 Tests with undissolved cathode pieces and whitish aluminum granules, while Figures 1(d)-1(f) depict #8, #10, and #11 Tests for which EDXRF measurements on the powder after dissolution reactions did not reveal the Al presence.

Table 2 shows the results of EDXRF measurements in the Tests #7 to #12 residues. As already announced in Table 1, among the cathodes in which the Al collector was visually dissolved (Tests #7 to #12), Al is still identified in the Tests #7 and #9 residues.

However, Ni, Mn, and Co were also identified in all six residues, with an average relative concentration of 56%, 23%, and 21%, respectively, accounting for the $LiNi_{0.56}Mn_{0.23}Co_{0.21}O_2$ composition of the cathode electroactive material of an NMC battery type.

Besides assessing the residue compositions by knowing their elements and relative weights through EDXRF, X-ray diffraction was also used to confirm the composition analytically, as shown in Figures 2(a) and 2(b). Using the X'Pert High Score Plus software on the X-ray diffraction data, the compounds $LiNi_{0.56}Mn_{0.23}Co_{0.21}O_2$ and $Al(OH)_3$ were identified in the residue #7 with relative weights of 79.0% and 21.0%, respectively.

The element Al in residue #7 was identified by EDXRF, Table 2, under the $Al(OH)_3$ compound. Residue #9 presented the same two compounds and weight proportions.

In the other residues, Tests #8, #10 to #12, only the $LiNi_{0.56}Mn_{0.23}Co_{0.21}O_2$ compound was identified, confirming the absence of cathode material contamination by aluminum, as concluded by EDXRF measurements in Table 1.

Figure 1 - Images of the residues of the cathode dissolution solutions: (a) Test #3, (b) Test #4, (c) Test #6, (d) Test #8, (e) Test #10, and (f) Test #11, as described in Table 1.

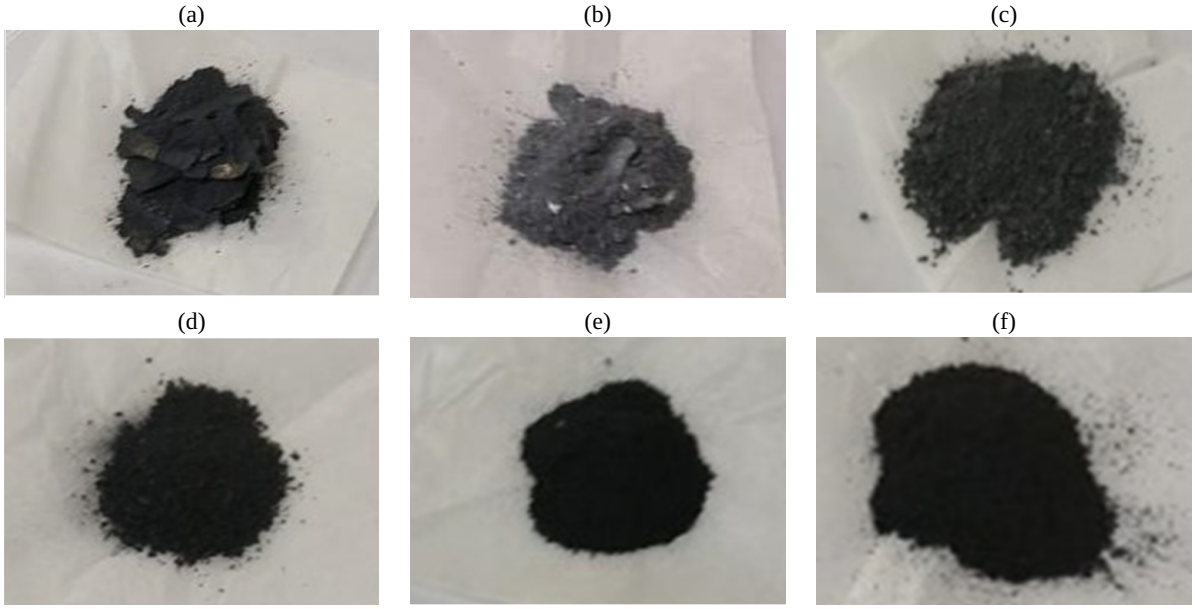

Figure 2 - Compositions and relative weights of residues, obtained from X-ray diffraction analyses, as described in Table 2: (a) Test #7, (b) Test #8.

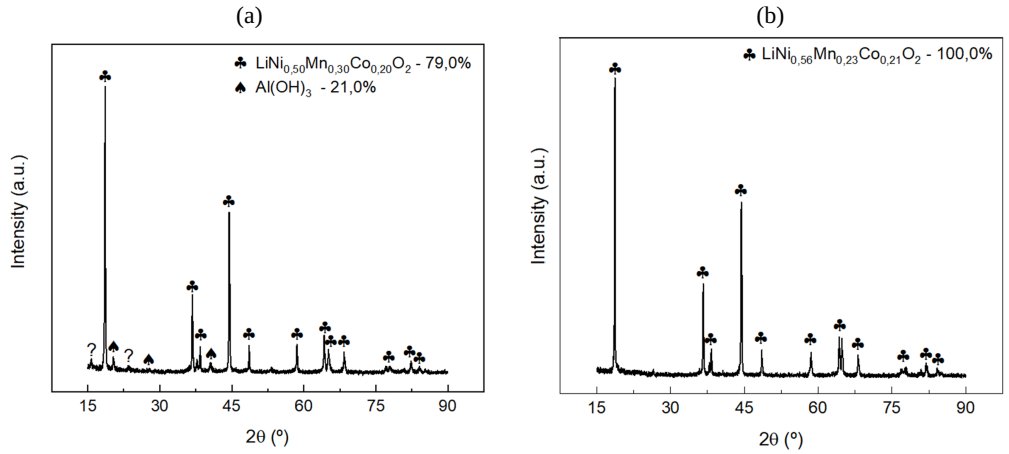

Detachment of material adhered to the separator

As mentioned, in LIBs opened individually or in batches of crushed batteries, it has often been observed that the polymeric separator becomes impregnated with the cathode material on one of its faces and anode material on the opposite face, as shown in Figure 3(a). It was observed that around 85% of the cathode and anode materials trapped in the two separator faces could be detached by the ultrasound cavitation process and an additional 5% by mechanical friction. Figure 3(b) shows an image of the separator after applying ultrasound and friction methods to the separator depicted in Figure 3(a). Approximately 90% of the electrode materials anchored in the separator were released, confirming the efficiency of the two-separation method.

The powder released from the separator is a mixture of the cathode material and C-graphite from the anode, as shown in Figure 4(a). The released cathode and anode materials were identified as $LiNi_{0.56}Mn_{0.23}Co_{0.21}O_2$ and graphite, with relative weights of 25.8% and 74.2%, respectively. The froth flotation technique can further separate the C-graphite from the cathode material (Zhan et al., 2018; Zhang et al., 2023). The detachment method described proved to be very suitable for recovering the electrode materials trapped in the fragments of crushed batteries. After filtering, the NaOH dissolution solution containing Al^{3+}, Na^{+}, H^{+}, and OH^{-} ions was evaporated, resulting in a white crystalline powder identified as Na_2CO_3, $NaAlO_2$, and AlO(OH) compounds from its X-ray diffractogram, as shown in Figure 4(b).

Figure 3 - Separator: (a) with anode and cathode materials adhered on its opposite faces, (b) after removal of materials by ultrasonic cavitation and mechanical friction.

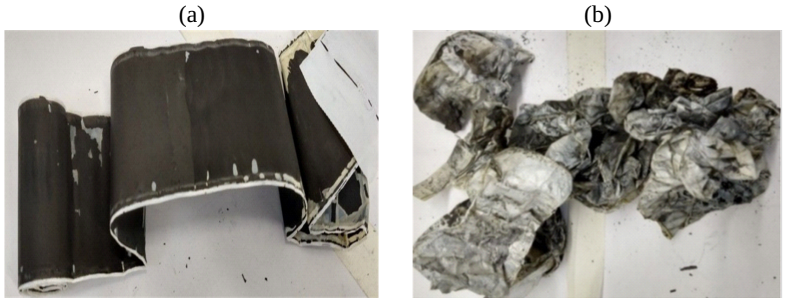

Figure 4 - Cathode and anode materials detached from the: (a) separator by ultrasound cavitation and mechanical friction methods; (b) compounds after evaporation of the NaOH dissolution solution.

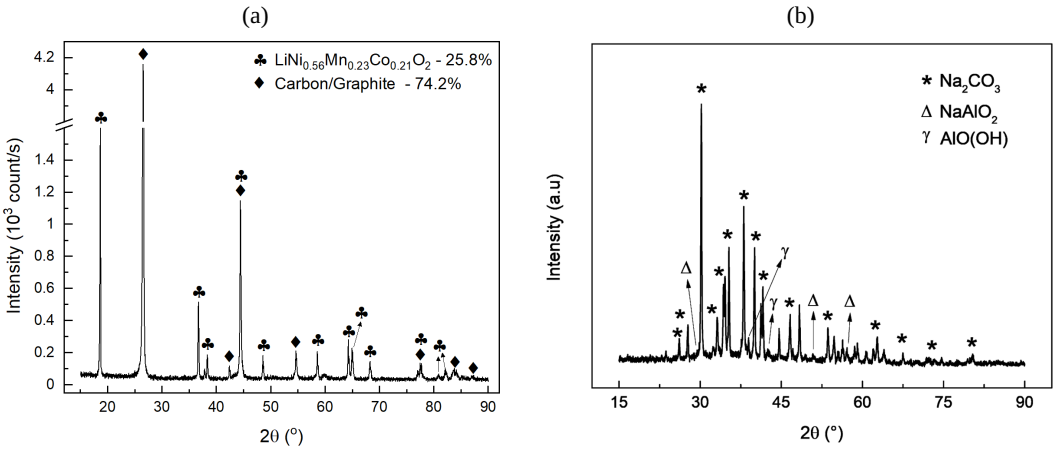

Battery discharges in $MnSO_4$ solution

Figure 5 shows the battery discharge curves as a function of the $MnSO_4$ solution concentration and reaction time.

In Figure 5(a), a discarded battery with a low residual charge (2.8 V) was discharged in a 0.5 mol L^{-1} $MnSO_4$ solution. In Figure 5(b), six discarded batteries were previously charged at 4.2 V and then discharged at 0.1, 0.5, and 1.0 mol L^{-1} concentrations in duplicate tests.

The voltage of the uncharged battery dropped from 2.8 V to 2.0 V in 48 min and to 1.5 V after almost two hours. Different behavior was observed for the batteries previously charged at 4.2 V: in the 0.1 mol L^{-1} $MnSO_4$ solution, a minimum battery voltage of 3.5 V was attained after 140 min of discharge. In 0.5 and 1.0 mol L^{-1}, the batteries were asymptotically discharged to a minimum of 2.0 V around 225 min. However, a discharge down to 2.5 V (considered deep) can be reached in 100 min in the 0.5 and 1.0 mol L^{-1} $MnSO_4$ solutions. It can be concluded that LIBs can be efficiently discharged in $MnSO_4$ solution to a minimum voltage, which depends on the residual battery state of charge and solution concentration. Moreover, the discharge curve profile depends on the concentration of the $MnSO^{-1}$ solution, as already reported by (Yao et al., 2020).

The results of Figure 5 can be understood in light of the electrochemical reactions of the ionic species of the solution medium on the surface of the battery poles. LIB discharge in the aqueous ionic solution occurs through water electrolysis reactions, with the $MnSO_4$ salt increasing the medium reactivity. However, secondary reactions also occur together with electrolysis, as shown.

In water electrolysis, hydroxyl anions, OH^-, are oxidized at the LIB positive pole surface, generating water and gaseous O_2, reactions in equation (1)

$$4OH^- \rightarrow 2H_2O + O_2(g) + 4e^-. \quad (1)$$

The released electrons reduce the cathode material of the LIB. Therefore, Li^+ ions from the electrolyte concomitantly diffuse into the cathode material to maintain its charge neutrality. In the LIB anode (cathode in electrolysis), H^+ and hydronium H_3O^+ cations of the solution are reduced, generating H_2, according to equations (2) and (3) reactions

$$2H^+ + 2e^- \rightarrow H_2(g), \quad (2)$$

$$2H_3O^+ + 2e^- \rightarrow 2H_2O + H_2. \quad (3)$$

Figure 5 - Battery voltage changes for discharges in $MnSO_4$ solutions: (a) of a battery with a low residual charge in the 0.5 mol L^{-1}, (b) six batteries previously charged at 4.2 V and discharged in 0.1, 0.5 and 1.0 mol L^{-1}.

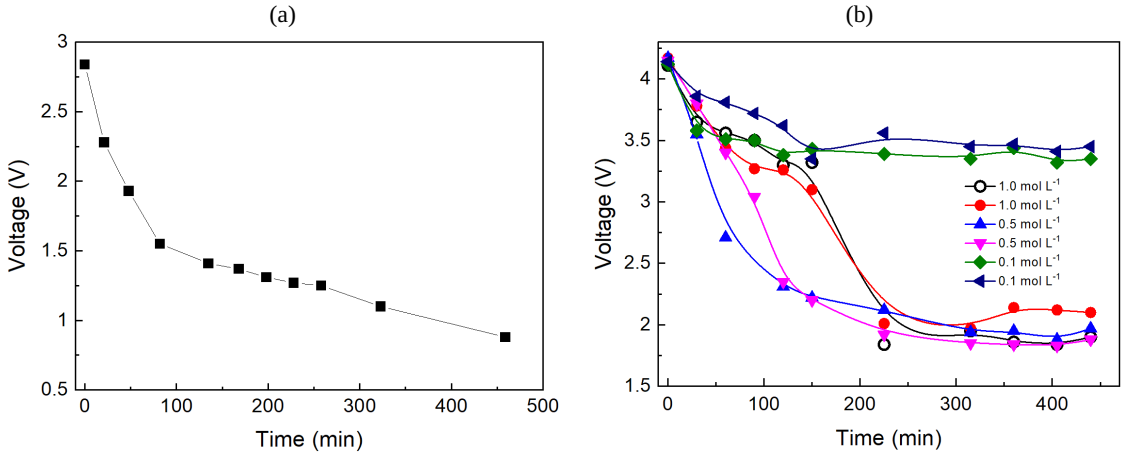

The reducing electrons come from the battery anode material; consequently, Li^+ ions are released into the battery electrolyte from the anode material. So, the water electrolysis reactions lead to the discharge of the LIB.

However, concomitant to the generation of O_2 carried out by the dissociation of water and subsequent reduction of OH^- described by the general reaction equation (4), two other reduction reactions occur on the surface of the cathode pole according to equations (5) and (6),

$$2H_2O \rightarrow 4H^+ + O_2 + 4e^- \qquad E^\circ = -1.30\,V, \quad (4)$$

$$Mn^{2+} \rightarrow Mn^{3+} + e^- \qquad E^\circ = -1.54\,V, \quad (5)$$

$$Fe \rightarrow Fe^{2+} + 2e^- \qquad E^\circ = +0.44\,V. \quad (6)$$

The oxidation of the Mn^{2+} cations occurs because the cathode potential is always above the standard electric potential (E^o) for this reaction. As the E^o of the reaction in equation (5) is close to the H_2O oxidation reaction equation (4), two competitive reactions take place on the cathode pole: one to produce O_2, reaction equation (4), and another to oxidize the Mn^{2+} cations from the solution to Mn^{3+}, reaction equation (5). The Mn^{3+} ions precipitate on the cathode pole surface as a thin amorphous layer, possibly as MnO_2 (Xiao et al., 2020). This insulating material progressively blocks the pole reactive area for the equations (4) and (5) reactions and, consequently, the equations (2) and (3) reactions at the anode pole.

In the third oxidation, Fe from the nickel-plated steel of the cathode pole suffers a galvanic dissociation, according to reaction equation (6), since the pole voltage is always above the 0.44 V of the standard potential of this reaction (A plastic covering protects the cylindrical surface of the battery case to redox reactions). The Fe^{2+} ions react with the medium products and precipitate as $Fe(OH)_2$ and $Fe(OH)_3$ (Xiao et al., 2020). The galvanic reaction equation (6) indirectly contributes to battery discharge. However, it damages the cathode pole by corrosion, which may lead to electrolyte leakage and solution entry into the battery, making it unfeasible for further recycling processes. Brown to black particles were visually observed in the becker after the battery discharge, presumably $Fe(OH)_3$ precipitates.

The three oxidation reactions at the battery cathode pole surface are concurrent and competitive with each other, generating gaseous O2, MnO2 layer over the pole, and $Fe(OH)_2$ and $Fe(OH)_3$ precipitate into the solution, as illustrated in Figure 6. All three reactions compete with H_2O products to react around the cathode surface, leading to battery discharge through their respective oxidation reactions in the cathode pole and reduction of H^+ to H_2 in the anode pole.

If the Mn^{2+} concentration is low, only part of the pole will be covered with the Mn oxide layer, as shown in Figure 6c, where a circular black necklace at the cathode edge is seen. O_2 releases and Mn oxidation continue to occur until deep corrosion in the cathode pole is established, leading to electrolyte leakage and, worst, OH^-, H_2O entry into the battery, neutralizing the counter ion Li^+ as LiOH or LiH and then rendering the battery inoperative. An acrid odor was smelled as soon as the battery was removed from the 0.1 mol L^{-1} solution after 440 min of discharging, indicating deep corrosion from which electrolyte leaked from the battery. This effect is claimed to explain why the battery voltage is kept at 3.5 V after 150 min of discharge when a 0.1 mol L^{-1} $MnSO_4$ solution was employed.

Under high concentrations of the $MnSO_4$ solution, the battery is initially discharged by three oxidation reactions at its cathode pole and the reduction at the anode pole. However, the high concentration of Mn^{2+} in the solution leads to a progressive coating of the cathode pole by the

Figure 6 - Effects of LIB discharge in MnO_2 solutions: (a) H_2 bubbles on the surface of the anode, (b) MnO_2 layer on the cathode surface, (c) corrosion of the cathode together with a ring of MnO_2 layer.

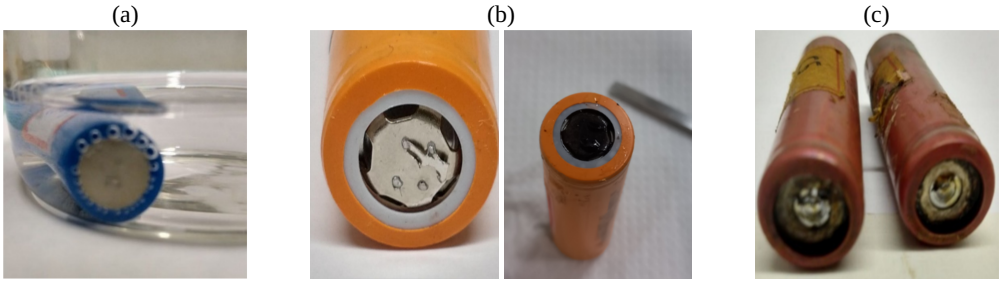

insulating MnO_2 layer at a rate enough to avoid deep corrosion and electrolyte leakage until the pole is fully covered, as shown in Figure 6b. After this, any oxidation reaction is not possible at the surface of the cathode pole, and the battery voltage is kept constant at 2.0 V after 225 min of discharge, as shown in Figure 5(b). No electrolyte leaking from the batteries was observed at the end of the discharge tests in these two concentrations.

While reactions occur at the cathode, the reaction to generate H_2 in the anode also occurs since H_2O (the source of OH^-) is generated and self-dissociated continually along the battery discharge reactions. Figure 6a shows the image of H_2 bubbles at the anode of a battery discharged in a 0.5 mol L^{-1} $MnSO_4$ solution.

Conclusions

To recover the cathode material firmly bonded to the aluminum collector and trapped in the separator of the Li-ion batteries, previous discharges in $MnSO_4$ solution were carried out. Three concurrent oxidation reactions occurred at the surface of the cathode pole, whose products were O_2, an insulating Mn-based layer on the pole surface, galvanic corrosion of the Fe of the nickel-plated steel pole, and the reduction of H^+ to H_2 in the battery anode pole were claimed to explain the discharge process.

The battery's lowest voltage attained in the discharges depended on the solution concentration and reaction time. Discharge at 0.1 mol L^{-1} resulted in corrosion of the cathode pole, electrolyte leakage, and the lowest voltage of 3.5 V. At 0.5 and 1.0 mol L^{-1}, the insulating Mn-based layer fully coated the cathode pole, and a 2.0 V lowest battery voltage was reached.

Ultrasonic cavitation in water could easily detach the cathode and anode materials incrusted into the separator. The cathode material was recovered by dissolving the Al collector in NaOH solution. A dependence of the dissolution efficiency on the NaOH solution concentration and the dissolution time was observed. Complete dissolution of the collector aluminum strips was found for NaOH solution above 1.5 mol L^{-1} in 1.0 h of reaction and at 1.25 and 1.50 mol L^{-1} concentrations after 4.0 h of dissolution reaction. Dissolutions by 1.0 h in these two last concentrations show the presence of $Al(OH)_3$ in the residue of the filtered solution. The cathode material was identified as the $LiNi_{0.56}Mn_{0.23}Co_{0.21}O_2$ compound by X-ray fluorescence and diffraction techniques.

Author contributions

M.H. Novaes participated in the investigation, validation, visualization, data curation, and writing (original draft); P.R.C. da Silva in formal analysis, and supervision; P.S. Parreira in the investigation (EDXRF); G.G. dos Santos in supervision; L. E. Sita in supervision and J. Scarminio participated in conceptualization, formal analysis, supervision, data curation and writing (revision and editing).

Conflicts of interest

The authors certify that there is no commercial or associative interest that represents a conflict of interest in relation to the manuscript.

Acknowledgments

M.H. Novaes, G.G. dos Santos, L.E. Sita, and J. Scarminio are grateful to CAPES and CNPq agencies for their scholarships and LARX/UEL research laboratory for providing access to the XRD and EDXRF equipment.

References

Asenbauer, J., Eisenmann, T., Kuenzel, M., Kazzazi, A., Chen, Z., & Bresser, D. (2020). The success story of graphite as a lithium-ion anode material fundamentals, remaining challenges, and recent developments including silicon (oxide) composites. *Sustainable Energy and Fuels*, *4*(11), 5387–5416. https://doi.org/10.1039/d0se00175a

Bae, H., & Kim, Y. (2021). Technologies of lithium recycling from waste lithium-ion batteries: A review. *Materials Advances*, *2*(10), 3234–3250. https://doi.org/10.1039/d1ma00216c

Bai, Y., Essehli, R., Jafta, C. J., Livingston, K. M., & Belharouak, I. (2021). Recovery of Cathode Materials and Aluminum Foil Using a Green Solvent. *ACS Sustainable Chemistry and Engineering*, *9*(17), 6048–6055. https://doi.org/10.1021/acssuschemeng.1c01293

Chen, T., Jin, Y., Lv, H., Yang, A., Liu, M., Chen, B., Xie, Y., & Chen, Q. (2020). Applications of Lithium-Ion Batteries in Grid-Scale Energy Storage Systems. *Transactions of Tianjin University*, *26*(3), 208–217. https://doi.org/10.1007/s12209-020-00236-w

Chen, Y., Kang, Y., Zhao, Y., Wang, L., Liu, J., Li, Y., Liang, Z., He, X., Li, X., Tavajohi, N., & Li, B. (2021). A review of lithium-ion battery safety concerns: The issues, strategies, and testing standards. *Journal of Energy Chemistry*, *59*, 83–99. https://doi.org/10.1016/j.jechem.2020.10.017

Ferreira, D. A., Prados, L. M. Z., Majuste, D., & Mansur, M. B. (2009). Hydrometallurgical separation of aluminum, cobalt, copper and lithium from spent Li-ion batteries. *Journal of Power Sources*, *187*(1), 238–246. https://doi.org/10.1016/j.jpowsour.2008.10.077

Gaye, N., Gueye, R. S., Ledauphin, J., Balde, M., Seck, M., Wele, A., & Diaw, M. (2019). Alkaline Leaching of Metals from Cathodic Materials of Spent Lithium-Ion Batteries. *Asian Journal of Applied Chemistry Research*, 1–7. https://doi.org/10.9734/ajacr/2019/v3i230088

He, Y., Yuan, X., Zhang, G., Wang, H., Zhang, T., Xie, W., & Li, L. (2021). A critical review of current technologies for the liberation of electrode materials from foils in the recycling process of spent lithium-ion batteries. *Science of the Total Environment*, *766*, 142382. https://doi.org/10.1016/j.scitotenv.2020.142382

Hu, H., Xue, W., Jiang, P., & Li, Y. (2022). Polyimide-Based Materials for Lithium-Ion Battery Separator Applications: A Bibliometric Study. *International Journal of Polymer Science*, *2022*(3). https://doi.org/10.1155/2022/6740710

Hu, Z., Zhu, N., Wei, X., Zhang, S., Li, F., Wu, P., & Chen, Y. (2021). Efficient separation of aluminum foil from mixed-type spent lithium-ion power batteries. *Journal of Environmental Management*, *298*, 113500. https://doi.org/10.1016/j.jenvman.2021.113500

Mahmud, S., Rahman, M., Kamruzzaman, M., Ali, M. O., Emon, M. S. A., Khatun, H., & Ali, M. R. (2022). Recent advances in lithium-ion battery materials for improved electrochemical performance: A review. *Results in Engineering*, *15*, 100472. https://doi.org/10.1016/j.rineng.2022.100472

Ojanen, S., Lundström, M., Santasalo-Aarnio, A., & Serna-Guerrero, R. (2018). Challenging the concept of electrochemical discharge using salt solutions for lithium-ion battery recycling. *Waste Management*, *76*, 242–249. https://doi.org/10.1016/j.wasman.2018.03.045

Shaw-Stewart, J., Alvarez-Reguera, A., Greszta, A., Marco, J., Masood, M., Sommerville, R., & Kendrick, E. (2019). Aqueous solution discharge of cylindrical lithium-ion cells. *Sustainable Materials and Technologies*, *22*, e00110. https://doi.org/10.1016/j.susmat.2019.e00110

Sita, L. E., dos Santos, C. S., da Silva, S. P., de Faria Lima, A., & Scarminio, J. (2022). A simple process to resynthesize the $LiCoO_2$ and $LiNi_{1/3}Co1/3Mn_{1/3}O_2$ compounds from the cathode material extracted from a batch of spent LCO batteries. *Journal of Alloys and Compounds*, *894*, 162350. https://doi.org/10.1016/j.jallcom.2021.162350

Sita, L. E., da Silva, S. P., da Silva, P. R. C., Urbano, A., & Scarminio, J. (2015). Optimization of $LiCoO_2$ powder extraction process from cathodes of lithium-ion batteries by chemical dissolution. *Semina: Ciências Exatas e Tecnológicas*, *36*(1), 11–18. https://doi.org/10.5433/1679-0375.2015v36n1p11

Torabian, M. M., Jafari, M., & Bazargan, A. (2022). Discharge of lithium-ion batteries in salt solutions for safer storage, transport, and resource recovery. *Waste Management and Research*, *40*(4), 402–409. https://doi.org/10.1177/0734242X211022658

Weng, Y., Xu, S., Huang, G., & Jiang, C. (2013). Synthesis and performance of $Li[(Ni_{1/3}Co_{1/3}Mn_{1/3})_{1-x}Mg_x]O_2$ prepared from spent lithium-ion batteries. *Journal of Hazardous Materials*, *246–247*, 163–172. https://doi.org/10.1016/j.jhazmat.2012.12.028

Xiao, J., Guo, J., Zhan, L., & Xu, Z. (2020). A Cleaner Approach to the Discharge Process of Spent Lithium-Ion Batteries in Different Solutions. *Journal of Cleaner Production*, *255*, 120064. https://doi.org/10.1016/j.jclepro.2020.120064

Yao, L. P., Zeng, Q., Qi, T., & Li, J. (2020). An Environmentally Friendly Discharge Technology to Pretreat Spent Lithium-Ion Batteries. *Journal of Cleaner Production*, *245*, 118820. https://doi.org/10.1016/j.jclepro.2019.118820

Zhan, R., Oldenburg, Z., & Pan, L. (2018). Recovery of Active Cathode Materials from Lithium-Ion Batteries Using Froth Flotation. *Sustainable Materials and Technologies*, *17*, e00062. https://doi.org/10.1016/j.susmat.2018.e00062

Zhang, J., Li, J., Wang, Y., Sun, M., Wang, L., & Tu, Y. (2023). Separation of Graphites and Cathode Materials from Spent Lithium-Ion Batteries Using Roasting–Froth Flotation. *Sustainability (Switzerland)*, *15*(1). https://doi.org/10.3390/su15010030

Zhong, X., Han, J., Chen, L., Liu, W., Jiao, F., Zhu, H., & Qin, W. (2021). Binding Mechanisms of PVDF in Lithium-Ion Batteries. *Applied Surface Science*, *553*, 149564. https://doi.org/10.1016/j.apsusc.2021.149564